Carbohydrate Polymers 82 (2010) 1284–1289

Contents lists available at ScienceDirect

Carbohydrate Polymers

journal homepage: www.elsevier.com/locate/carbpol

# Thermal degradation kinetics of chitosan–cobalt complex as studied by thermogravimetric analysis

Chun-Yan Ou[a], Chao-Hua Zhang[b], Si-Dong Li[a,*], Lei Yang[a], Jing-Jing Dong[a], Xue-Liu Mo[a], Mu-Ting Zeng[a]

[a] College of Science, Guangdong Ocean University, Zhanjiang 524088, People's Republic of China
[b] College of Food Science and Technology, Guangdong Ocean University, Zhanjiang 524088, People's Republic of China

ARTICLE INFO

*Article history:*
Received 19 February 2010
Received in revised form 30 April 2010
Accepted 2 July 2010
Available online 13 July 2010

*Keywords:*
Chitosan–cobalt complex
Chitosan
Thermogravimetric analysis
Degradation mechanism
Kinetic parameter

ABSTRACT

The thermal degradation of chitosan–cobalt complex at different heating rates in nitrogen was studied by thermogravimetric analysis (TGA) in the temperature range 30–800 °C. Fourier transform-infrared (FTIR) and X-ray diffractogram (XRD) analyses were utilized to determine the micro-structure of chitosan–cobalt complex. The results indicate that the thermal degradation of chitosan–cobalt complex in nitrogen is a two-step reaction, characteristic temperatures and the maximum reaction rate of thermal degradation increase with the increment of heating rate. The kinetic parameters were determined by using Friedman and Flynn–Wall–Ozawa methods. Coats–Redfern method was used to discuss the probable degradation mechanism. The results show that activation energy of the complex resulting from two kinetic methods has similar variable tendency, and the solid-state decomposition in the first degradation stage, which is non-spontaneous, goes to a mechanism involving nucleation and growth, Avrami–Erofeev function ($A_4$) with integral form $[-\ln(1-\alpha)]^4$.



## 1. Introduction

Chitosan (CTS), the most abundant natural amino polysaccharide, is produced by the deacetylation of chitin which is one of the key constituents of the shells of crustaceans and by-product of the fishing industry. Chitosan is flexible, insoluble in the vast majority of solvents but capable of being cast into films and fibers from dilute acid (Liu, Li, Lv, Wu, & Li, 2005; Shih & Fung, 2006). One of the major applications of chitosan is based on its ability that adsorbs metal ions through ion exchange or chelation mechanisms, because of the presence of nucleophilic functional groups, such as hydroxyl, amino and its high nitrogen content (Domard, 1987; Felse & Panda, 1999; Juang, Wu, & Tseng, 1999; Rachakornkij, Ruangchuaya, & Teachakulwiroj, 2004; Ruiz, Sastre, & Guibal, 2000). Recently, increasing attention has been paid to the use of chitosan and its derivatives that supported metal complexes as catalysts of industrial processes. For example, chitosan–cupric (II) complex could serve as an initiator for vinyl monomer (Inaki, Otsuru, & Takemoto, 1978), chitosan–Schiff base cobalt (II) and palladium (II) complexes could be catalysts in the oxidation of cyclohexane (Tong, Li, & Xia, 2005), quaternary ammonium salt covalently bound to chitosan is an efficient and recyclable single-component catalyst for the synthesis of propylene carbonate (Zhao, Tian, & Qi, 2007). During the use of the catalyst, reaction conditions such as pressure, temperature, etc. will seriously affect the catalytic activity, so the study of their thermal stability is very important. Unfortunately, there are few reports about the kinetics of thermal degradation of chitosan–metal complex. In this article, the thermal degradation of chitosan–cobalt complex is investigated with dynamic thermogravimetric analysis (TGA). The objective is to study the kinetics of the thermal degradation of chitosan–cobalt complex using different kinetic methods under non-isothermal condition.

## 2. Theoretical background

The application of dynamic TG methods holds great promise as a tool for unraveling the mechanism of physical and chemical processes that occur during polymer degradation. In general, the thermal degradation of a solid polymer can be simply shown as: $B_{solid} \rightarrow C_{solid} + D_{gas}$ where $B_{solid}$ is the initial material, $C_{solid}$ and $D_{gas}$ are the different products during the disappearance of $B_{solid}$. In thermogravimetric measurements, the degree of decomposition (conversion) can be calculated as follows:

$$\alpha = \frac{W_0 - W_T}{W_0 - W_f} \quad (1)$$

* Corresponding author. Tel.: +86 13702737491; fax: +86 759 2383636.
*E-mail address:* lisidong2210491@yahoo.com.cn (S.-D. Li).

0144-8617/$ – see front matter © 2010 Elsevier Ltd. All rights reserved.
doi:10.1016/j.carbpol.2010.07.010

where $\alpha$ is extent of decomposition; $W_T$, $W_0$, $W_f$ are the actual, initial and final mass of the sample, respectively. A typical model for a kinetic process can be expressed as:

$$-\frac{d(1-\alpha)}{dt} = Kf(\alpha) \quad (2)$$

where $-d(1–\alpha)/dt$ is the decomposition rate; $f(\alpha)$, the function of $\alpha$, depends on the particular decomposition mechanism. $K$ is the decomposition rate constant, which is assumed to obey the Arrhenius relationship:

$$K = A\exp\left(\frac{-E_\alpha}{RT}\right) \quad (3)$$

where $A$ is the pre-exponential factor ($s^{-1}$), $E_\alpha$ is the activation energy (kJ mol$^{-1}$), $R$ is the gas constant (8.314 J mol$^{-1}$ K$^{-1}$) and $T$ is the absolute temperature (K). Substituting the Eq. (3) into Eq. (2), we obtain

$$-\frac{d(1-\alpha)}{dt} = A\exp\left(\frac{-E_\alpha}{RT}\right)f(\alpha) \quad (4)$$

If the temperature of a sample is changed by a constant value of $\beta$ ($\beta = dT/dt$), the variation of the degree of decomposition can be analyzed as a function of temperature. Therefore, the decomposition rate gives:

$$-\frac{d(1-\alpha)}{dT} = \frac{A}{\beta}\exp\left(\frac{-E_\alpha}{RT}\right)f(\alpha) \quad (5)$$

The Eqs. (4) and (5) are the basic equations for the kinetic calculation.

### 2.1. Friedman method (Friedman, 1964)

This method is a differential method, and it is based on Eq. (5) whose logarithm is:

$$\ln\left(\frac{d\alpha}{dt}\right) = \ln\left(\beta\frac{d\alpha}{dT}\right) = \ln[Af(\alpha)] - \frac{E_\alpha}{RT} \quad (6)$$

From this equation, it is easy to obtain values for $E_\alpha$ over a wide range of conversions by plotting $\ln[\beta(d\alpha/dT)]$ against $1/T$ at constant value of $\alpha$. The slope of each line is $-E_\alpha/R$.

### 2.2. Flynn–Wall–Ozawa method

This method is an integral method. Separating the variable, rearranging and integrating Eq. (5), it can be obtained:

$$g(\alpha) = \int_{\alpha_0}^{\alpha_p}\frac{d\alpha}{f(\alpha)} = \frac{A}{\beta}\int_{\alpha_0}^{\alpha_p}\exp\left(\frac{-E_\alpha}{RT}\right)dT \quad (7)$$

If we define $x = E_\alpha/RT$ and integrate the right-hand side of Eq. (7), it can be obtained:

$$\frac{A}{\beta}\int_{\alpha_0}^{\alpha_p}\exp\left(\frac{-E_\alpha}{RT}\right)dT = \frac{AE_\alpha}{\beta R}p(x) \quad (8)$$

After taking logarithms, we obtain:

$$\log\beta = \log\frac{AE_\alpha}{g(\alpha)R} + \log p(x) \quad (9)$$

using the Doyle approximation (Reich & Stivala, 1971), the function $p(x)$ can be expressed as the following approximation:

$$\log p(x) = -2.315 - 0.4567x \quad (10)$$

Substituting Eq. (10) to Eq. (9), it can be obtained:

$$\log\beta = \log\frac{AE_\alpha}{g(\alpha)R} - 2.315 - \frac{0.4567E_\alpha}{RT} \quad (11)$$

Eq. (11) is the formula of Flynn–Wall–Ozawa method (Lyon, 1997; Sun, Huang, Gong, & Cao, 2006). From this equation, it is easy to obtain values for $E_\alpha$ over a wide range of decomposition by plotting $\log\beta$ against $1/T$ at constant value of $\alpha$. The slope of each line is $-0.4567\ E_\alpha/(RT)$, without knowledge of the reaction order.

### 2.3. Coats–Redfern method (Coats & Redfern, 1964; Tomaszewicz & Kotfica, 2004)

The Coats–Redfern method uses an asymptotic approximation for the resolution of Eq. (7) at different conversion values. If $(2RT)/E_\alpha \to 0$ is true for the Doyle approximation, a natural logarithmic form can be obtained:

$$\ln\frac{g(\alpha)}{T^2} = \ln\frac{AR}{\beta E_\alpha} - \frac{E_\alpha}{RT} \quad (12)$$

According to the different degradation processes, with the theoretical function $g(\alpha)$ being listed in Table 1 (Urbanovici, Popescu, & Seqal, 1999), $E_\alpha$ and $A$ can be obtained from the plot of $\ln[g(\alpha)/T^2]$ versus $1/T$, as well as the valid reaction mechanism.

## 3. Experimental

### 3.1. Materials

#### 3.1.1. Chitosan

Chitosan was obtained from Shanghai Greenbird Science and Technology Development Co. Ltd. (Shanghai, China), and its viscosity average molecular weight was 180 kDa, the degree of deacetylation of chitosan was >90%.

#### 3.1.2. Synthesis of chitosan–cobalt complex

A mixture of 30 mL 1% acetic acid and 500 mg chitosan in a beaker was magnetically stirred at 25 °C for 1 h, then 500 mg cobalt chloride dissolved in 60 mL distilled water was slowly added into the beaker, stirred for 5 h. 1% Sodium carbonate aqueous solution was then slowly added, until the pH value of the solution was adjusted to 8.0. The reaction was stopped. The chitosan–cobalt complex was precipitated, filtered, washed several times with water and ethanol, then dried under vacuum oven.

### 3.2. Characterization of samples

#### 3.2.1. FTIR analysis

A PerkinElmer Spectrum-GX-1 infrared spectrometer was used to obtain FTIR data. FTIR spectra were recorded in the wave number range of 4000–400 cm$^{-1}$ with a resolution of 4 cm$^{-1}$.

#### 3.2.2. X-ray diffraction

X-ray diffraction patterns of samples were measured by a D/max IIIA diffractometer (Rigaku, Japan) and used a Cu Kα target at 35 kV and 25 mA.

#### 3.2.3. Thermogravimetric analysis

Thermogravimetric analysis was performed on a TG/DTA6300 system (Seiko Instruments, Japan Tokyo). The measuring accuracy of sample temperature was checked by the onset fusion temperatures of indium (156.6 ± 0.2 °C) and Sn (232 ± 0.2 °C) with heating/cooling dynamic segments. In this work, the mass of each sample was 5–6 mg. The carrier gas was nitrogen at a flow rate of 50 mL min$^{-1}$. The samples were heated from 30 to 800 °C at various values of $\beta$ (5, 10, 15, 20, 25 °C min$^{-1}$) to record the TGA and differential thermogravimetric analysis (DTG) curves. The experiments were repeated thrice to confirm the repeatability and authenticity of the generated data.

**Table 1**
Algebraic Expressions for $g(\alpha)$ for the most frequently used mechanisms of solid-state processes.

| Symbols | $g(\alpha)$ | Solid-state processes |
|---|---|---|
| Sigmoidal curves | | |
| $A_2$ | $[-\ln(1-\alpha)]^2$ | Nucleation and growth (Avrami equation (1)) |
| $A_3$ | $[-\ln(1-\alpha)]^3$ | Nucleation and growth (Avrami equation (2)) |
| $A_4$ | $[-\ln(1-\alpha)]^4$ | Nucleation and growth (Avrami equation (3)) |
| Deceleration curves | | |
| $R_1$ | $\alpha$ | Phase boundary controlled reaction (one-dimensional movement) |
| $R_2$ | $2[1-\ln(1-\alpha)^{1/2}]$ | Phase boundary controlled reaction (contracting area) |
| $R_3$ | $3[1-\ln(1-\alpha)^{1/3}]$ | Phase boundary controlled reaction (contracting volume) |
| $D_1$ | $\alpha^2$ | One-dimensional diffusion |
| $D_2$ | $(1-\alpha)\ln(1-\alpha)+\alpha$ | Two-dimensional diffusion (Valensi equation) |
| $D_3$ | $[1-(1-\alpha)^{1/3}]^2$ | Three-dimensional diffusion (Jander equation) |
| $D_4$ | $[1-(2/3)\alpha]-(1-\alpha)^{2/3}$ | Three-dimensional diffusion (Ginstlinge–Brounshtein equation) |
| $F_1$ | $-\ln(1-\alpha)$ | Random nucleation with one nucleus on the individual particle |
| $F_2$ | $1/(1-\alpha)$ | Random nucleation with two nuclei on the individual particle |
| $F_3$ | $1/(1-\alpha)^2$ | Random nucleation with three nuclei on the individual particle |

## 4. Results and discussion

### 4.1. FTIR analysis

Fig. 1 shows the FTIR spectra of the chitosan and chitosan–cobalt complex. The characteristic FTIR bands of samples are listed in Table 2. For chitosan, a strong and broad absorbent band centered at 3452.9 $cm^{-1}$ is attributed to –OH asymmetrical stretching vibration and $-NH_2$ stretching vibration (Sajomsang, Gonil, & Tantayanon, 2009). There are two absorption bands at 2960–2850 $cm^{-1}$, which are attributed to –C–H stretching of the alkyl substituent (Britto & Assis, 2007), The absorption band at 1634.6 $cm^{-1}$ is assigned as amide I vibrations (Cai, Song, Shang, & Yang, 2007; Li, Du, Wu, & Zhan, 2004). The absorption band at 1406.9 $cm^{-1}$ is caused by the coupling of –C–N– stretching vibration, and the band which appears at 1083.4 $cm^{-1}$ corresponds to the stretching of –C–O– bond. The absorption band at 661.4 $cm^{-1}$ is resulted from –N–H stretching vibration (Yin, Yuan, Lin, Tan, & Zhang, 2006). FTIR spectrum of chitosan–cobalt complex shows the similar bands of chitosan, and it exhibits an intense set of bands in the low-frequency region (650–400 $cm^{-1}$), these bands are ascribed to stretching vibrations of Co–N, Co–O bonds (Mekahlia & Bouzid, 2009). In addition, a significant decrease of wave numbers is observed in absorptions of amide I vibrations, –C–O– stretching vibration, the coupling of –C–N– stretching vibration and –N–H stretching vibration. The intensity of amide I vibrations and –C–O– stretching vibration become weak, which suggest an effective coordination between chitosan and cobalt ion via amine and hydroxyl functional groups.

### 4.2. X-ray diffraction

From Fig. 2, it is seen that chitosan shows two characteristic peaks of crystalline nature at $2\theta$ of 9.85°, 19.70°, but the chitosan–cobalt complex is characterized by a broad amorphous peak at 20.67°. Thus, complexation of cobalt leads to very significant changes in the morphology of the chitosan, indicating complete disruption of the interpolymer bonds.

### 4.3. TG analysis

#### 4.3.1. Effect of $\beta$ on the process of thermal degradation of chitosan–cobalt complex

Fig. 3 is the TG and DTG curves of thermal degradation of chitosan–cobalt complex at five different heating rates in nitrogen. The test at heating rate of 10 °C $min^{-1}$ was repeated thrice to confirm the repeatability and authenticity of the generated data. The average relative deviation (ARD) value of chitosan–cobalt complex is 2.17. The average relative deviation is defined as:

$$\mathrm{ARD}(\%) = \frac{100}{NJ}\sum_{i=1}^{N}\sum_{j=1}^{J}\left|\frac{W_{T_i}-\overline{W_{T_i}}}{\overline{W_{T_i}}}\right| \quad (13)$$

where $W_{T_i}$ is mass fraction of the sample at the temperature $T_i$, $\overline{W_{T_i}}$ is the average mass fraction of the sample at the temperature $T_i$, $J$ is experiment times, $N$ is the number of data points.

It can be seen that there are three peaks on the DTG curves. The first peak appears round 100 °C, which is related to water loss in the material. So, chitosan–cobalt complex is degraded in two stages corresponding to the second peak and the third peak respec-

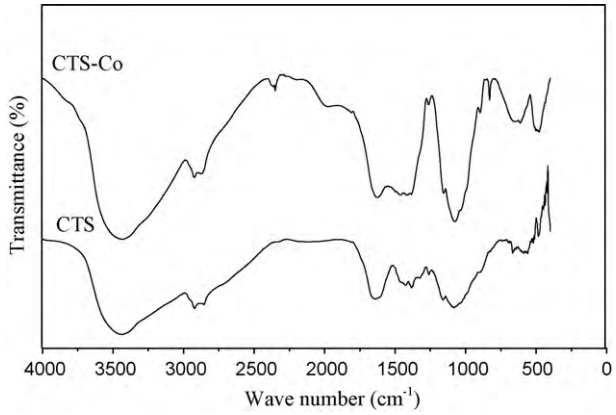


**Fig. 1.** Infrared spectra of chitosan and chitosan–cobalt complex.

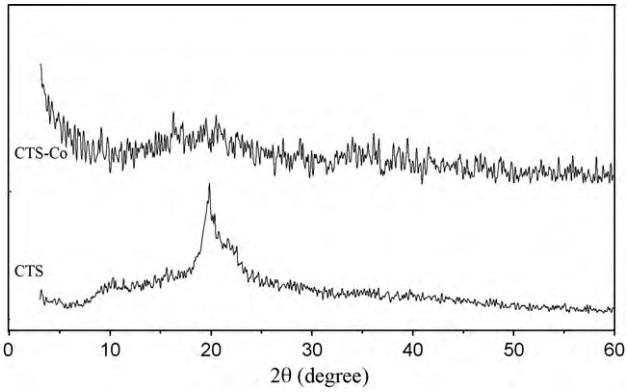


**Fig. 2.** X-ray diffraction patterns of chitosan and chitosan–cobalt complex.

**Table 2**
Characteristic FTIR bands of chitosan and chitosan–cobalt complex.

| Samples | FTIR ($cm^{-1}$) |
|---|---|
| CTS | 3452.9 (–OH, $–NH_2$), 2932.5 (C–H), 2874.9 (C–H), 1634 .6 ($–NH_2$), 1406.9 (–C–N–), 1083.4 (C–O–), 661.4 (N–H) |
| CTS–Co | 3452.9 (–OH, $–NH_2$), 2932.5 (C–H), 2874.9 (C–H), 1627 .4 ($–NH_2$), 1401.2 (C–N), 1076.2 (C–O–), 655.2 (N–H), 478.2 (Co–N, Co–O) |

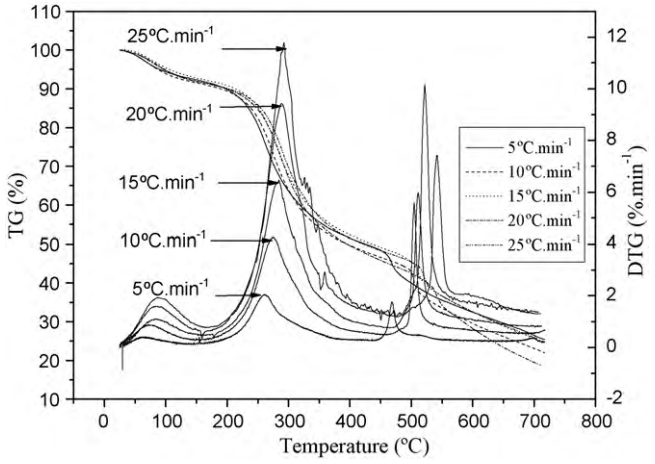


**Fig. 3.** TG and DTG curves of the thermal degradation of chitosan–cobalt complex.

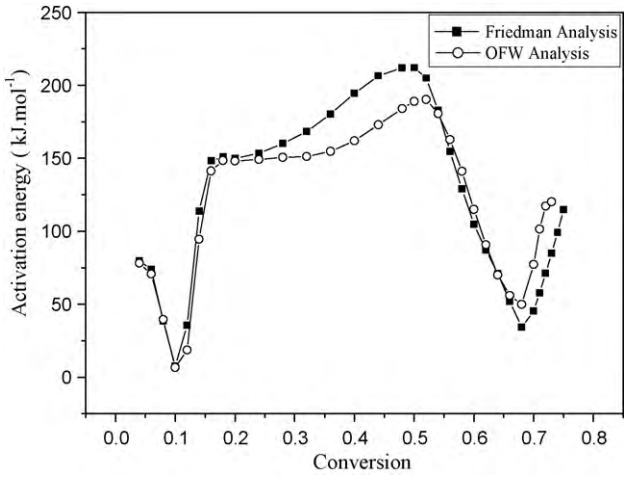


**Fig. 4.** Activation energies of chitosan–cobalt complex obtained by Friedman method and by Flynn–Wall–Ozawa method.

tively. The characteristic temperatures for the two stages of thermal degradation of chitosan–cobalt complex are given in Table 3. $T_{st}$ is the temperature of initial weight loss and $T_{max}$ is the temperature at maximum weight loss rate, that is the peak temperature on a differential thermogravimetry curve.

The first thermal degradation process occurs in the temperature range 160–400 °C. The second thermal degradation process occurs in the temperature range 400–700 °C. All the degradation temperatures increase linearly with the increasing of $\beta$, indicating that the degradation temperatures are mainly affected by $\beta$. The relations between $\beta$ and $T$ are as follows: $T_{st,1} = (1.008\beta + 166.2)$ °C ($r = 0.9904$), $T_{max,1} = (1.550\beta + 256.9)$ °C ($r = 0.9649$) (the first stage); $T_{st,2} = (3.570\beta + 424.7)$ °C ($r = 0.9919$), $T_{max,2} = (2.7\beta + 470.0)$ °C ($r = 0.8457$) (the second stage), where $r$ is the correlation coefficient. The linear increment of thermal degradation temperatures along with the increasing of $\beta$ is a result of the heat hysteresis (Coats & Redfern, 1963; Herbell, 1972). To eliminate the heat hysteresis, the thermal degradation temperature should be expressed in equilibrium thermal degradation temperature ($T^0$) which is the temperature when $\beta$ approaches 0. The equilibrium thermal degradation temperatures of chitosan are as follows: $T^0_{st,1} = 166.2$ °C, $T^0_{st,2} = 424.7$ °C, $T^0_{max,1} = 256.9$ °C, $T^0_{max,2} = 470.0$ °C. The peak height of the DTG curve, that is, the maximum reaction rate of thermal degradation ($R_p$), increases with the increasing of $\beta$, The relationship between $\beta$ and $R_p$ is as follows: $R_{p,1} = (-0.589 + 0.486\beta)$ %·min$^{-1}$ ($r = 0.9984$) (the first stage); $R_{p,2} = (0.453 + 0.374\beta)$% min$^{-1}$ ($r = 0.9719$) (the second stage).

*4.3.2. The determination of activation energy of chitosan–cobalt complex*

Friedman method, which is a most widely used differential method and independent of any thermal degradation mechanism, was firstly employed to analyze the TG data of chitosan–cobalt complex. Friedman method is based on Eq. (6) and requires several thermograms (at least four) at different heating rates. The values of activation energy were determined from plots of $\ln(\beta(d\alpha/dT))$ against $1/T$, obtained from each thermogram at constant values of $\alpha$. A set of straight lines was obtained at different conversion, with the slope of each line being $-E_\alpha/R$. The calculated results are illustrated in Fig. 4.

Flynn–Wall–Ozawa method is an integral method, and independent of the degradation mechanism. Eq. (11) was used, and the activation energy of chitosan–cobalt complex was obtained from plot of log $\beta$ against $1000/T$ at a fixed conversion with the slope of such a line being $-0.4567E_\alpha/(RT)$. The activation energies calculated from the slopes are also shown in Fig. 4.

Through analyzing the activation energies obtained by the two methods, it was found that the variable tendency of $E_\alpha$ was similar to each other, which can be divided into three weight-loss phases: 0–0.10, 0.20–0.50, and 0.55–0.75. At the first stage, $E_\alpha$ is small, this may be due to the volatilization of low-molecular-weight materials such as water. After that, $E_\alpha$ increase slightly along with increasing degree of decomposition (145–210 kJ mol$^{-1}$ for Friedman method and 140–190 kJ mol$^{-1}$ for Flynn–Wall–Ozawa method), this may be caused by the deacetylation of the main chain and the cleavage of glycosidic linkages of chitosan. During the last stage, which

**Table 3**
Characteristic temperatures for the thermal degradation of chitosan–cobalt complex.

| Heating rate (°C min$^{-1}$) | The first stage (160–400 °C) | | The second stage (400–700 °C) | |
|---|---|---|---|---|
| | $T_{st}$ (°C) | $T_{max}$ (°C) | $T_{st}$ (°C) | $T_{max}$ (°C) |
| 5 | 171.6 | 260.9 | 442.6 | 473.4 |
| 10 | 174.8 | 274.3 | 461.9 | 504.3 |
| 15 | 182.9 | 284.3 | 473.4. | 510.7 |
| 20 | 186.2 | 288.4 | 501.0 | 542.2 |
| 25 | 191.1 | 292.6 | 512.3 | 522.0 |

**Table 4**
Kinetic parameters during the first thermal degradation stage of chitosan–cobalt complex.

| $\beta$ (°C min$^{-1}$) | $E_\alpha$ (kJ mol$^{-1}$) | $A$ (s$^{-1}$) | $\Delta H$ (kJ mol$^{-1}$) | $\Delta S$ (J mol$^{-1}$ K) | $\Delta G$ (kJ mol$^{-1}$) |
|---|---|---|---|---|---|
| 5 | 140.6 | $7.9 \times 10^7$ | 145.0 | −98.6 | 197.6 |
| 10 | 142.9 | $1.9 \times 10^8$ | 147.4 | −91.6 | 197.6 |
| 15 | 152.7 | $1.3 \times 10^9$ | 157.4 | −75.3 | 199.4 |
| 20 | 151.9 | $1.7 \times 10^9$ | 156.6 | −73.7 | 197.9 |
| 25 | 149.7 | $8.6 \times 10^8$ | 154.4 | −79.2 | 199.2 |

contributes to the thermal destruction of pyranose ring and the decomposition of the residual carbon, $E_\alpha$ decreases firstly and then increases, and this may be two opposite results of cobalt ion catalyzing the thermal destruction of pyranose ring and disturbing the decomposition of the residual carbon (Ou et al., 2008). Therefore, the suggestion that the values obtained from these two methods determine the range of $E_\alpha$ is reasonable.

#### 4.3.3. Determination of kinetic mechanisms of chitosan–cobalt complex

Compared to other methods, these two methods (Friedman and Flynn–Wall–Ozawa) present the advantage that they do not require previous knowledge of the reaction mechanism for determining the activation energy. Some researches (Montserrat, Málek, & Colomer, 1998; Núñez, Fraga, Núñez, & Villanueva, 2000) used the activation energies obtained by these two methods to check their thermal degradation mechanism models. To investigate the solid-state process for the first thermal degradation of chitosan–cobalt complex (the second thermal degradation is not discussed because of complexity of $E_\alpha$ according to Friedman and Flynn–Wall–Ozawa methods), Coats–Redfern method was chosen.

Coats–Redfern equation is based on Eq. (12). The assignment of the mechanism of thermal decomposition is based on the assumption that the form of $g(\alpha)$ depends on the reaction mechanism. Correlation coefficients for all these forms were calculated and the form of $g(\alpha)$ for which the correlation has a maximum value is selected as the mechanism reaction. In this investigation, thirteen forms of $g(\alpha)$ were used, in order to enunciate the mechanism of thermal decomposition. One thermal decomposition parameter, activation entropy, was determined from equation: $A = kT_{max}/h\, e^{\Delta S/R}$ (Gabal, 2003), where $k$ is the Boltzmann constant ($1.38 \times 10^{-23}$ J K$^{-1}$), $h$ is the Planck constant ($6.63 \times 10^{-34}$ J s) and $T_{max}$ is the temperature related to DTG peak value determined from Fig. 3, listed in Table 3. The other thermal degradation parameter, the activation enthalpy was obtained from the following equation: $E_\alpha = \Delta H - RT_{max}$ (Faria & Prado, 2007). Finally, the activation Gibbs energy was calculated from equation: $\Delta G = \Delta H - T_{max}\Delta S$ (Faria and Prado, 2007).

For the chitosan–cobalt complex, the best value of correlation coefficient in the first thermal degradation stage was obtained using this function $[-\ln(1-\alpha)]^4$, which corresponds to a mechanism involving nucleation and growth. All kinetic thermal degradation parameters calculated from thermogravimetric curves are listed in Table 4.

Kinetic thermal analysis shows that the $E_\alpha$ obtained by Coats–Redfern method is in good agree with that obtained by Friedman and Flynn–Wall–Ozawa methods. And all $E_\alpha$, $\Delta H$, and $\Delta G$ values are positive and $\Delta S$ values are negative, consequently, indicating non-spontaneous process of the first decomposition of chitosan–cobalt complex.

## 5. Conclusions

The thermal degradation of chitosan–cobalt complex in nitrogen is a two-stage reaction. The degradation temperature increases along with the increment of heating rate. The maximum reaction rate of thermal degradation increases with the increasing of heating rate. The kinetic parameters involved in the thermal degradation of chitosan–cobalt complex were investigated by using Friedman method and Flynn–Wall–Ozawa method. The results show that the variable tendency of $E_\alpha$ is similar to each other, and $E_\alpha$ can be divided into three weight-loss phases corresponding to the volatilization of low-molecular-weight materials such as water, the deacetylation of the main chain and the cleavage of glycosidic linkages of chitosan, the thermal destruction of the pyranose ring and the decomposition of the residual carbon, respectively. The results obtained by Coats–Redfern method show that the solid-state process for the first degradation stage of chitosan–cobalt complex is non-spontaneous and goes to a mechanism involving nucleation and growth, Avrami–Erofeev function ($A_4$) with integral form $[-\ln(1-\alpha)]^4$.

## References


Britto, D., & Assis, B. G. O. (2007). Synthesis and mechanical properties of quaternary salts of chitosan-based films for food application. *International Journal of Biological Macromolecules*, *41*, 198–203.

Cai, Z. S., Song, Z. Q., Shang, S. B., & Yang, C. S. (2007). Study on the flocculating properties of quaternized carboxymethyl chitosan. *Polymer Bulletin*, *9*, 655–665.

Coats, A. W., & Redfern, J. P. (1963). Thermogravimetric analysis: A review. *Analyst*, *88*, 906–924.

Coats, A. W., & Redfern, J. P. (1964). Kinetic parameters from the thermogravimetric data. *Nature (London)*, *201*, 68–69.

Domard, A. (1987). pH and c.d. measurements on a fully deacetylated chitosan: Application to Cu (II)–polymer interactions. *International Journal of Biological Macromolecules*, *9*(4), 98–104.

Faria, E. A., & Prado, A. G. S. (2007). Kinetic studies of the thermal degradation of cellulose acetate/niobium and chitosan/niobium composites. *Reactive and Functional Polymers*, *67*, 655–661.

Felse, P. A., & Panda, T. (1999). Studies on applications of chitin and its derivatives. *Bioprocess Engineering*, *20*, 505–512.

Friedman, H. (1964). Kinetics of thermal degradation of char-forming plastics from thermogravimetry. Application to a phenolic plastic. *Journal of Polymer Science: Part C*, *6*, 183–195.

Gabal, M. A. (2003). Kinetics of the thermal decomposition of $CuC_2O_4$–$ZnC_2O_4$ mixture in air. *Thermochimica Acta*, *402*, 199–208.

Herbell, T. P. (1972). *Thermochimica Acta*, *4*, 295.

Inaki, Y., Otsuru, M., & Takemoto, K. (1978). Vinyl polymerization by metal complexes. XXXI. Initiation by chitosan–copper (II) complex. *Journal of Macromolecular Science*, *12*(7), 953–970.

Juang, R. S., Wu, F. C., & Tseng, R. L. (1999). Adsorption removal of copper (II) using chitosan from simulated rinse solutions containing chelating agents. *Water Research*, *33*(10), 2403–2409.

Li, H. B., Du, Y. M., Wu, X. J., & Zhan, H. Y. (2004). Effect of molecular weight and degree of substitution of quaternary chitosan on its adsorption and flocculation properties for potential retention-aids in alkaline papermaking. *Colloids and Surfaces A: Physicochemistry. English Aspects*, *242*, 1–8.

Liu, Y. H., Li, Y. X., Lv, J., Wu, G. D., & Li, J. B. (2005). Graft copolymerization of methyl methacrylate onto chitosan initiated by potassium ditelluratocuprate (III). *Journal of Macromolecular Science Pure and Applied Chemistry*, *42*, 1169–1180.

Lyon, R. E. (1997). An integral method of non-isothermal kinetic analysis. *Thermochimica Acta*, *297*, 117–124.

Mekahlia, S., & Bouzid, B. (2009). Chitosan–copper (II) complex as antibacterial agent: Synthesis, characterization and coordinating bond-activity correlation study. *Physics Procedia*, *2*, 1045–1053.

Montserrat, S., Málek, J., & Colomer, P. (1998). Thermal degradation kinetics of epoxy-anhydride resins: I. Influence of a silica filler. *Thermochimica Acta*, *313*, 83–95.

Núñez, L., Fraga, F., Núñez, M. R., & Villanueva, M. (2000). Thermogravimetric study of the decomposition process of the system BADGE ($n = 0$)/1, 2 DCH. *Polymer*, *41*, 4635–4641.

Ou, C. Y., Li, S. D., Li, C. P., Zhang, C. H., Yang, L., & Chen, C. P. (2008). Effect of cupric ion on thermal degradation of chitosan. *Journal of Applied Polymer Science*, *109*, 957–962.

Rachakornkij, M., Ruangchuaya, S., & Teachakulwiroj, S. (2004). Removal of reactive dyes from aqueous solution using bagasse fly ash. *Journal of Science and Technology*, *26*, 13–24.

Reich, L., & Stivala, S. S. (1971). *Elements of polymer degradation*. New York: McGraw-Hill.

Ruiz, M., Sastre, A. M., & Guibal, E. (2000). Palladium sorption on glutaraldehyde-crosslinked chitosan. *Reactive and Functional Polymers*, *45*, 155–173.

Sajomsang, W., Gonil, P., & Tantayanon, S. (2009). Antibacterial activity of quaternary ammonium chitosan containing mono or disaccharide moieties: Preparation and characterization. *International Journal of Biological Macromolecules*, *44*, 419–427.

Shih, F. Y., & Fung, K. Z. (2006). Effect of chitosan addition on the electrochemical behavior and crystallization of $LiMn_2O_4$ film derived from acetates-containing solution. *Electrochimica Acta*, *51*, 6533–6541.

Sun, J. T., Huang, Y. D., Gong, G. F., & Cao, H. L. (2006). Thermal degradation kinetics of poly (methylphenylsiloxane) containing methacryloyl groups. *Polymer Degradation and Stability*, *91*, 339–346.

Tomaszewicz, E., & Kotfica, M. (2004). Mechanism and kinetics of thermal decomposition of nickel (II) sulfate (VI) hexahydrate. *Journal of Thermal Analysis and Calorimetry*, *77*(1), 25–31.

Tong, J. H., Li, Z., & Xia, C. G. (2005). Highly efficient catalysts of chitosan–Schiff base Co (II) and Pd (II) complexes for aerobic oxidation of cyclohexane in the absence of reductants and solvents. *Journal of Molecular Catalysis A: Chemical*, *231*, 197–203.

Urbanovici, E., Popescu, C., & Seqal, E. (1999). Improved interactive version of the Coats–Redfern method to evaluate non-isothermal kinetic parameters. *Journal of Thermal Analysis and Calorimetry*, *58*, 683–700.

Yin, X. Q., Yuan, W., Lin, Q., Tan, Y. P., & Zhang, Q. (2006). Low molecular weight chitosan prepared from oxidative degradation of chitosan–Cu (II) complex. *Chinese Journal of Applied Chemistry*, *23*, 729–733.

Zhao, Y., Tian, J. S., & Qi, X. H. (2007). Quanternary ammonium salt-functionalized chitosan: A easily recyclable catalyst for efficient synthesis of cyclic carbonates from epoxides and carbon dioxide. *Journal of Molecular Catalysis A: Chemical*, *271*, 284–289.